Genomics 98 (2011) 164–172

Contents lists available at ScienceDirect

Genomics

journal homepage: www.elsevier.com/locate/ygeno

A functional *in vivo* screen for regulators of tumor progression identifies HOXB2 as a regulator of tumor growth in breast cancer

Pamela J. Boimel, Cristian Cruz, Jeffrey E. Segall *

Department of Anatomy and Structural Biology, Albert Einstein College of Medicine of Yeshiva University, Bronx, NY 10461, USA

ARTICLE INFO

Article history:
Received 11 December 2010
Accepted 28 May 2011
Available online 13 June 2011

Keywords:
shRNA
Functional screen
Breast cancer
Homeobox 2

ABSTRACT

Microarray profiling in breast cancer patients has identified genes correlated with prognosis whose functions are unknown. The purpose of this study was to develop an *in vivo* assay for functionally screening regulators of tumor progression using a mouse model. Transductant shRNA cell lines were made in the MDA-MB-231 breast cancer line. A pooled population of 25 transductants was injected into the mammary fat pads and tail veins of mice to evaluate tumor growth, and experimental metastasis. The proportions of transductants were evaluated in the tumor and metastases using barcodes specific to each shRNA transductant. We characterized the homeobox 2 transcription factor as a negative regulator, decreasing tumor growth in MDA-MB-231, T47D, and MTLn3 mammary adenocarcinoma cell lines. Homeobox genes have been correlated with cancer patient prognosis and tumorigenesis. Here we use a novel *in vivo* shRNA screen to identify a new role for a homeobox gene in human mammary adenocarcinoma.

1. Introduction

Breast cancer is the most common malignancy and the second most common cause of cancer related death in women. Ninety percent of deaths from tumors are due to metastasis, making the pathophysiology of this process and the study of genes involved in regulating metastasis central to advancing our understanding of this disease [1]. Oncogenes and tumor suppressor genes have been an important focus of study and drug design, as both metastasis growth and significant tumor burden contribute to poor clinical outcome. However individually evaluating these genes is time consuming. Screens can expedite functional validation of many proposed oncogenes and tumor suppressors in order to identify potential drug candidates. Breast cancer microarray studies have attempted to characterize the prognostic profile and therapeutic sensitivities of patients. Expression signatures predicting clinical outcome have correlated microarray studies with breast cancer patient prognosis [2–5]. The results of these studies, as well as those used in the clinical setting, indicate that clinical microarray data may provide large numbers of candidate genes to be evaluated for their contributions to both tumor growth and metastasis [6,7].

Developing a high-throughput *in vitro* screen based on shRNA lentiviral vectors has been previously demonstrated [8,9]. In those studies, genes were down-regulated in cells using shRNAs in a pooled population and placed under an *in vitro* outgrowth assay to select for genes regulating *in vitro* tumor cell growth. Although *in vitro* studies allow for rapid evaluation and selection of a large number of target genes, they neglect the importance of the tumor microenvironment. The screen we developed uses *in vivo* assays for breast cancer cell growth in the primary tumor and seeding and growth of lung metastases after tail vein injection to select for genes regulating these processes. Similarly, an *in vivo* screen for tumor suppressors in liver cancer used shRNA pools to identify and validate tumor suppressor genes in a liver mouse model [10]. Formation and growth of the tumor as well as the metastatic cascade are complex processes involving extensive input from the microenvironment and supporting stroma, making *in vivo* studies imperative for functional characterization of genes.

In this study we detected changes in the proportions of individual cell lines within a pooled population compared to the original injected pool proportions after selection for *in vivo* primary tumor growth in the mammary fat pad or seeding and growth in the lungs after experimental metastasis. We found that the HOXB2 transcription factor acts as a negative tumor growth regulator, decreasing proliferation in mammary adenocarcinoma tumors.

2. Results

2.1. Experimental design

To develop this screen we chose to evaluate genes correlated with patient prognosis across three breast cancer microarray analyses

Abbreviations: genomic DNA, gDNA.

* Corresponding author. Fax: +1 718 678 1019.
E-mail address: jeffrey.segall@einstein.yu.edu (J.E. Segall).

0888-7543/$ – see front matter © 2011 Elsevier Inc. All rights reserved.
doi:10.1016/j.ygeno.2011.05.011

[2,4,5]. We generated a pooled population of twenty-five individual shRNA transductant cell lines using the breast cancer line MDA-MB-231 clone 4173, previously identified as being highly metastatic to the lungs [11]. Each shRNA transductant cell line was made separately as a pool of transductants generated from a pGipz shRNA lentiviral vector designed to downregulate expression of a selected gene. The pGipz vector (from Open Biosystems) contains a CMV promoter driving expression of GFP, a puromycin resistance gene, and an shRNA off a single mRNA using an IRES sequence. Since the GFP and shRNA are present on the same mRNA, GFP levels could be used to estimate shRNA expression. The GFP levels of transductant pools with different targeted genes were similar, indicating similar levels of shRNA expression (Supplemental Fig. 1). Each vector contains a unique 60 base pair barcode sequence which was used to identify the integrated vector and determine the proportion of the transductants carrying that vector in the population in the screen. Knock-down of the targeted gene in each of the 25 shRNA transductant cell lines was evaluated by quantitative Real Time-PCR, qRT-PCR, of cDNA with primer sets to each gene. Up to four shRNA vectors were evaluated for knockdown of the targeted gene, and the shRNA cell lines with the highest knockdown for each gene were selected (Supplemental Tables 1 and 2). Multiple shRNA cell lines per gene were included in the screen if there was more than one shRNA with high knockdown. To make the pooled population of shRNA transductants, equal numbers of cells of each of the 25 shRNA transductant cell lines were combined. In order to detect changes in the proportion of each individual shRNA transductant in the pool, specific qRT-PCR primers to the unique 60 base pair barcode sequences in each of the 25 vectors were designed and tested. A common forward primer was used to hybridize to the vector DNA in between the shRNA and the barcode and a specific reverse primer was designed for each of the individual unique 60 bp barcodes (Supplemental Table 3). SYBR green qRT-PCR was done to determine the initial proportion of each individual transductant's DNA within the pool.

2.2. In vivo screen for regulators of tumor growth and metastasis

For the *in vivo* screen, the shRNA pool was either injected into the mammary fat pads of female SCID mice to identify tumor growth regulators or injected via tail vein to identify regulators of lung seeding and growth (Fig. 1). Genomic DNA, gDNA, was isolated from the pool for later comparison with the *in vitro* and *in vivo* grown samples. The pool was also grown *in vitro* in parallel. After four weeks the lungs were removed from the tail vein injected mice and at six weeks the primary tumors were removed. The tumors and lungs were dissociated, plated and tumor cells were selected using the puromycin resistance present in the pGipz vector. The *in vitro* cultures grown in parallel were similarly treated. gDNA was isolated and SYBR green qRT-PCR done using the barcode specific primers to look at the change in the relative proportion of each individual transductant within the total pool. The average proportion of each of the individual transductant cell lines within the pool after *in vivo* and *in vitro* growth was compared to the initial pool proportions (Table 1, and Fig. 2). If the proportion of a cell line increased in the pool after growth in the primary tumor or lung metastases, then the gene targeted by the corresponding shRNA potentially inhibits tumor growth and/or metastasis. If the proportion of a cell line decreased in the pool after growth in the primary tumor or lung metastases, then the targeted gene potentially stimulates tumor growth and/or metastasis.

ANOVA analysis of the relative proportions of the individual transductants before and after *in vitro* growth indicated a significant change ($p<.031$). Examining the individual transductants' proportions after *in vitro* growth identified 7 genes (CBFB, COL4A5, CYBA, ID1, MPHOSPH6, PTPN14, and SERPINE1) whose proportions in the pool were significantly reduced after *in vitro* growth (*t* test, $p<.05$). ANOVA analysis of the *in vivo* samples showed more significant changes ($p<10^{-19}$ and .0021, respectively, for primary tumor growth and lung growth). For primary tumor growth, 12 transductants showed proportions that were significantly altered. Transductants

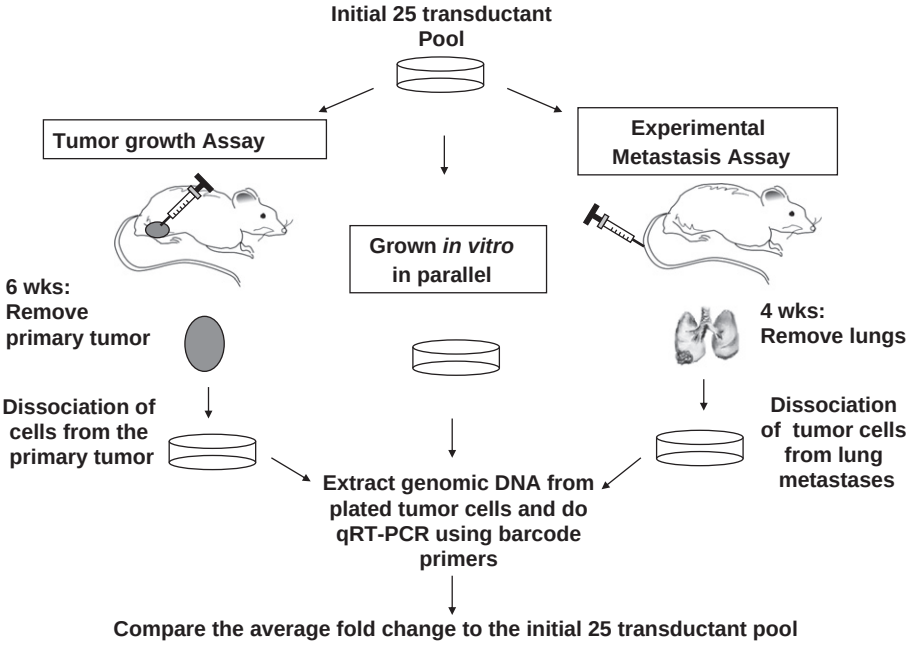

Fig. 1. Experimental design of screen. The pool of transductants was injected into the right 4th mammary fat pad of female SCID mice (Tumor Growth Assay) to screen for *in vivo* tumor growth regulators and into the tail vein of female SCID mice (Experimental Metastasis Assay) to screen for metastasis regulators. The pool was also grown *in vitro* in parallel and genomic DNA isolated at the same time point as the *in vivo* samples. For mammary fat pad injections, after 6 weeks the primary tumor was removed and tumor cells were dissociated and plated in puromycin containing medium to select for tumor cells. For tail vein injections, after 4 weeks the lungs were removed and lung metastases were dissociated and tumor cells plated and plated in puromycin containing medium to select for tumor cells. The parallel *in vitro* grown cells were also puromycin treated. Genomic DNA was isolated from puromycin resistant cultures, and specific barcode primers were used to evaluate the change in proportion of each of the individual transductants in the samples compared to the proportions in the initial injected pool sample.

Table 1
Summary of screen results.

	In vitro	p	Primary	p	Lung	p
BAI2-B	0.68	4.10E−01	0.76	5.06E−01	0.60	1.38E−01
CBFB-B	0.52	1.65E−01	1.53	5.83E−01	**0.32**	**1.31E−03**
CBFB-C	**0.32**	**2.60E−02**	0.96	8.59E−01	**0.39**	**1.70E−02**
CEBPB-E	0.99	9.88E−01	0.69	2.88E−01	1.34	2.76E−01
CELSR2-A	0.94	7.89E−01	**0.26**	**5.73E−04**	1.26	5.61E−01
COL4a5-B	**0.36**	**4.27E−02**	**0.31**	**2.36E−07**	0.68	3.90E−01
CT1	1.86	2.30E−01	**9.89**	**1.28E−02**	1.08	8.70E−01
CYBA-B	**0.33**	**1.78E−02**	**0.11**	**5.81E−08**	0.93	7.13E−01
EGFR	0.78	5.26E−01	0.86	5.42E−01	2.14	3.12E−01
EREG	1.01	9.79E−01	**0.35**	**2.41E−05**	1.09	1.11E−01
HIF1A-D	1.31	4.23E−01	0.94	7.02E−01	1.82	6.08E−02
HOXB2-A	1.26	3.80E−01	**6.75**	**1.93E−02**	1.66	4.01E−01
ID1-C	**0.24**	**1.74E−02**	**0.12**	**8.40E−09**	0.68	3.78E−01
IGF1R-B	0.83	6.93E−01	1.56	1.91E−01	0.86	2.17E−01
IGF1R-D	0.90	3.87E−01	0.93	8.64E−01	0.53	1.72E−01
IL13RA2	0.49	6.87E−02	0.74	3.79E−01	1.42	1.40E−01
MPHOSPH6	**0.20**	**1.36E−02**	**0.26**	**2.46E−05**	1.35	4.56E−01
MTX2	1.26	3.19E−01	2.21	3.04E−01	0.75	8.47E−02
PTPN14-D	**0.38**	**3.33E−02**	1.34	1.91E−01	1.13	4.66E−01
RHOC	2.32	4.20E−01	0.67	1.82E−01	**1.57**	**2.18E−02**
RLN2-A	0.55	1.48E−01	0.82	7.01E−01	0.57	7.32E−02
SERPINE1-B	**0.50**	**4.37E−02**	0.59	1.54E−01	0.77	2.34E−01
STC2-C	0.87	6.76E−01	**0.19**	**3.89E−07**	**0.62**	**2.09E−02**
TGFBI-C	0.89	3.71E−01	**0.39**	**1.30E−02**	**0.67**	**3.18E−03**
VCAM1-B	0.77	5.89E−01	**0.37**	**1.86E−02**	0.74	5.82E−01
VCAM1-C	1.00	9.98E−01	**0.30**	**3.39E−04**	0.79	2.83E−01

Legend. Changes in proportion of each shRNA transductant cell line in the screen. Data shown are average change in proportion compared to the initial transductant pool for growth *in vitro* (N = 3), primary tumor growth (N = 9), and experimental lung metastasis (N = 3). p Values are *t* tests against a reference constant value of 1 (no change in proportion). Items in bold type correspond to a p value of <.05.

whose proportions were altered in both the *in vitro* growth and primary tumor were COL4A5, CYBA, ID1, and MPHOSPH6, (Fig. 3). Of the transductants whose proportions were altered only in the primary tumor, CELSR2, EREG, and VCAM1 (2 different shRNAs) showed reduced proportions after growth in the primary tumor, while HOXB2 and the line expressing what is described by Open Biosystems as a non-targeting shRNA (CT1) showed increased proportions. Transductants whose proportions were altered both in the primary tumor and experimental lung metastases were STC2 and TGFBI (both decreased), while the RHOC transductant showed a slight increase in lung metastasis. Two independent CBFB shRNA transductants were reduced both in the *in vitro* growth and lungs but not in the primary tumor (Fig. 3).

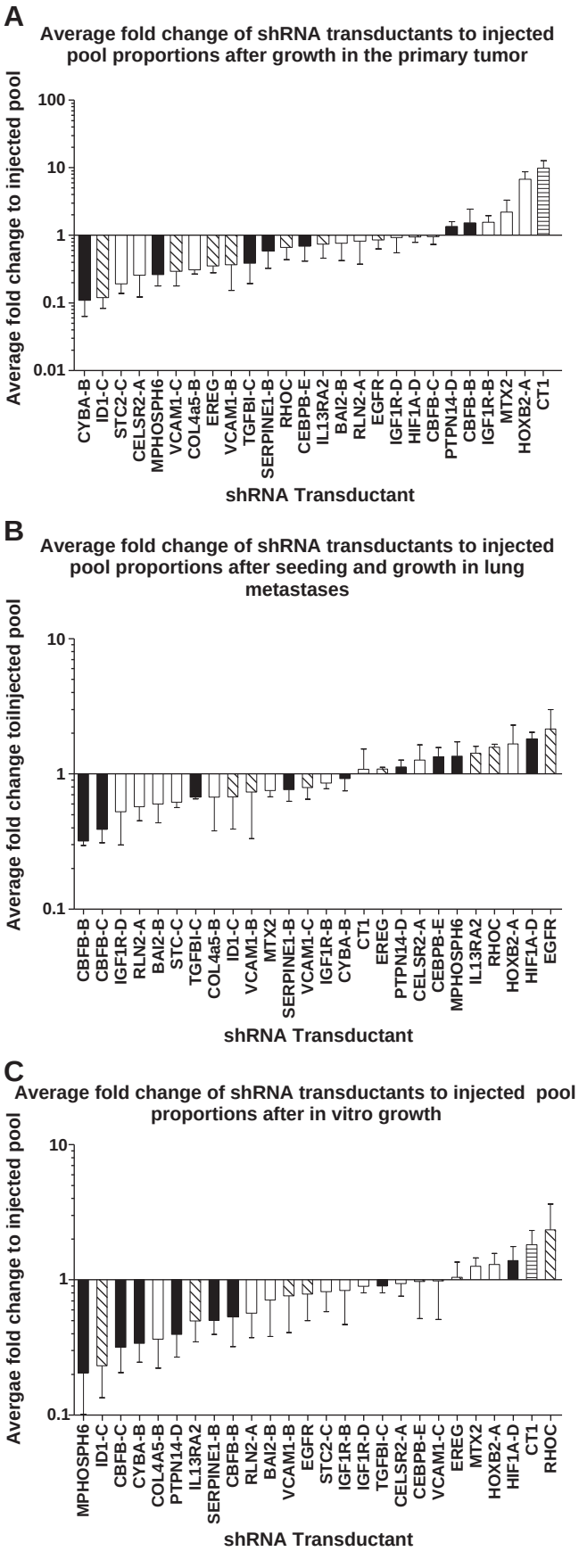

Fig. 2. *In vivo* screen for regulators of tumor growth and metastasis. Bars of potential growth/metastasis enhancers are black, potential growth/metastasis suppressors are white, controls (previously published positive enhancers of metastasis) are in a diagonal stripe pattern, and the non-targeting shRNA CT-1 is in a horizontal stripe pattern. (A) Average fold change of shRNA transductants after growth in the primary tumor. Nine female SCID mice were injected in the mammary fat pad with 1×10^6 cells of the initial pool. After 6 weeks tumors were removed, dissociated with collagenase, hyaluronidase, and DNase I and plated under puromycin selection. Genomic DNA was isolated from the cells and used to determine the average fold change in proportion to the initial pool using qRT-PCR with specific barcode primer sets. Means and SEM of results from primary tumors from 9 mice are plotted. (B) Average fold change of shRNA transductants after seeding and growth in lung metastases. 1×10^6 cells of the initial pool were injected in PBS into the lateral tail vein of female SCID mice. After 4 weeks, lungs were extracted and dissociated with collagenase, hyaluronidase, and DNase I and metastases plated under puromycin selection. Genomic DNA was isolated from the cells and used to determine the average fold change in proportion to the initial pool using qRT-PCR with specific barcode primer sets. Mean and SEM are plotted for results from 3 separate mice. (C) Average fold change to injected pool proportions after *in vitro* growth. The initial pool was grown *in vitro* and split 1:5, 3 times per week over 6 weeks (two separate 6 week *in vitro* growth measurements were done of the initial pool, over the time period of the two separate *in vivo* tumor injections). Genomic DNA was isolated at 4 and 6 weeks, and used to determine the average fold change in proportion to the initial pool using qRT-PCR with specific barcode primer sets. The average was taken of the fold change from the 4 week, and two 6 week isolations. Means and SEM of the data are plotted.

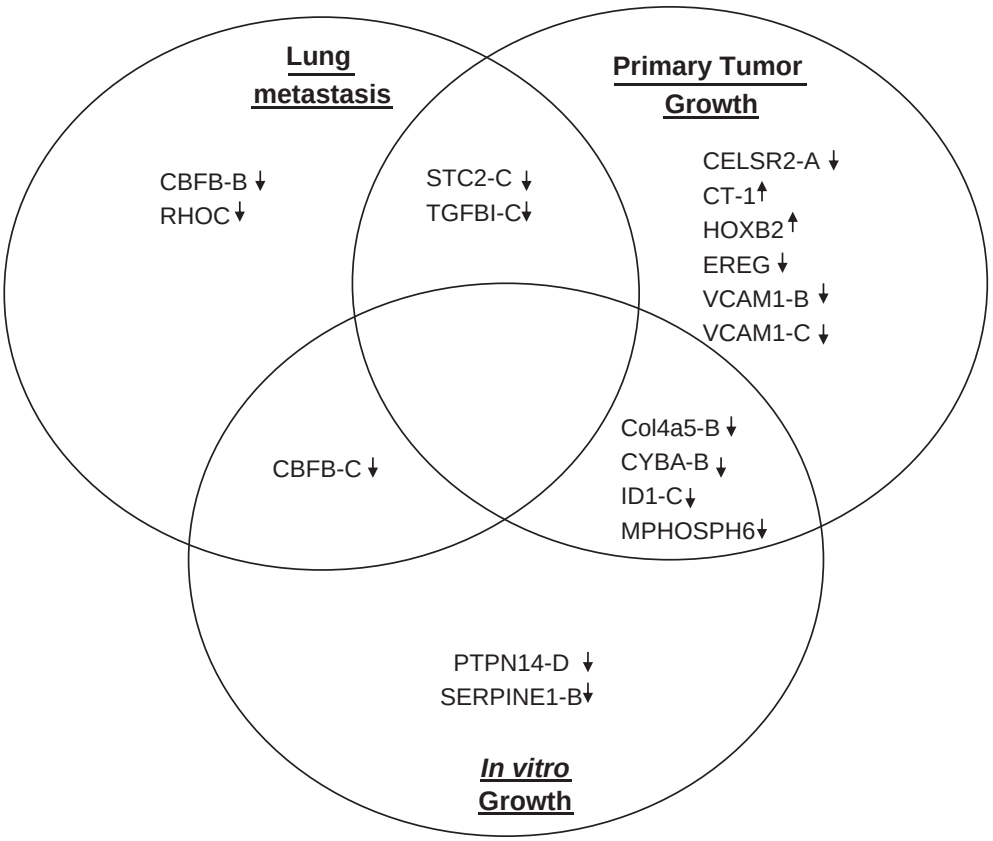

Fig. 3. Relationships between transductants with significant changes in representation. For genes that were significantly altered in the screen, the effect of knockdown on transductant representation in the pool is indicated by arrows (down indicates reduced representation and up indicates increased representation). The genes are organized according to the selection under which their representation is altered.

Of the potential positive effector targets, the inhibitor of DNA binding (ID1) shRNA transductant decreased in all conditions, and significantly in the *in vitro* and primary tumor samples. The epiregulin (EREG) shRNA transductant decreased significantly only in the primary tumor samples. For the vascular cell adhesion molecule, (VCAM1), there were two different shRNA transductants and both decreased significantly in the primary tumor. The EGFR and RHOC transductants did not show any significant changes. The most surprising result was the dramatic increase in the non-targeting shRNA (CT1) line in primary tumor growth (Fig. 2A).

2.3. HOXB2 is a negative growth regulator

We then tested selected lines that were identified in the screen to determine their individual *in vivo* growth properties, and proliferative and invasive capacity *in vitro*. We had found that the non-targeting CT1 cell line increased in proportion in the tumor growth screen, indicating that it had off-target effects. We therefore proceeded using SERPINE1-A, which had no knockdown of its targeted gene (Supplemental Table 1), as an alternative control. The CBFB-C shRNA cell line was tail vein injected to evaluate if it would have decreased lung seeding and growth compared to the parental line or the SERPINE1-A control cell line. There was no significant difference in the number of total lung metastases between the parental, SERPINE1-A, or CBFB-C cell lines (Fig. 4). CBFB knockdown also had no effect on *in vitro* invasion or proliferation compared to the SERPINE1-A control line (Supplemental Figs. 2 and 3).

To evaluate genes indicated to regulate growth in the *in vivo* primary tumor screen we injected shRNA cell lines individually into the mammary fat pads of female SCID mice to measure tumor growth curves. We tested the lines which had the most dramatic fold change compared to the initial injected pool proportions as well as TGFBI, which specifically decreased in proportion after *in vivo* tumor growth and not after *in vitro* growth. Tumor growth for the CYBA and TGFBI shRNA transductant cell lines, evaluated individually, indicated no significant difference in the number of days it took for the average tumor volume to reach 1000 mm^3 compared to either the MDA-MB-

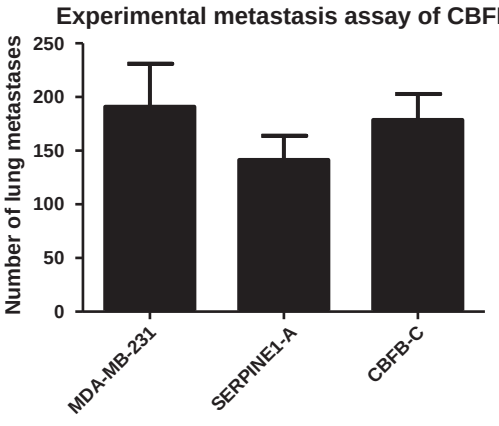

Fig. 4. The CBFB shRNA cell line is not altered in lung metastasis. The MDA-MB-231 parental cell line, SERPINE1-A, and CBFB-C shRNA cell lines were evaluated for seeding and growth in the lungs after tail vein injection. 2.5×10^5 cells were injected into the lateral tail vein of female SCID mice for each cell line. After 3 weeks lungs were formalin fixed, sectioned and H&E stained, and the number of lung metastases was counted. Mean and SEM are plotted for measurements from 5 mice for each cell line. There were no significant differences.

Table 2
Tumor growth of individual pGipz cell lines.

Cell line	Days to grow 1000 mm^3 tumor	Number of mice
MDA-MB-231 parental	47 (+/−3 days)	5
pGipz CT-1	35 (+/−2 days) ($p = 0.023658$)	4
pGipz CYBA-B	48 (+/−2 days)	6
pGipz TGFBI-C	44 (+/−3 days)	3
pGipz SERPINE1-A (alternate control)	44 (+/−3 days)	10
pGipz HOXB2-A	33 (+/−2 days) ($p = 0.001011$)	9

Legend. 1×10^6 cells were injected into the mammary fat pads of female SCID mice. Tumors were measured every 3 days for up to 58 days and the mean and SEM number of days to reach a tumor volume of 1000 mm^3were calculated. p Values for cell lines whose tumor growth was significantly different from the SERPINE1-A control shRNA line are provided. Mean and SEM are shown for the given number of separate mouse injections.

231 parental or Serpine1-A control cell lines (Table 2). Similar to the characterization of the individual cell line *in vivo*, knockdown of CYBA had no effect on the *in vitro* proliferation or invasive capacity of this cell line (Supplemental Figs. 2 and 3). The CT1 shRNA cell line tumors grew at a significantly accelerated rate compared to the other cell lines, consistent with its increase in proportion in the screen after tumor growth (Table 2).

The HOXB2 shRNA cell line tumors grew more rapidly, taking 33 days to reach an average tumor volume of 1000 mm^3, consistent with the increase in proportion in the screen after tumor growth (Table 2, and Fig. 5A). Knockdown of HOXB2 in the T47D human mammary adenocarcinoma cell line also increased tumor growth significantly compared to the SERPINE1-A control (Supplemental Fig. 4). This confirmed the screen result that HOXB2 may be a tumor growth suppressor and we further evaluated this possibility by overexpressing the HOXB2 open-reading frame in the JP1520 vector in both MDA-MB-231 and the rat mammary adenocarcinoma cell line MTLn3-ErbB1 [12]. There was no significant difference in *in vitro* growth of the HOXB2 shRNA and ORF cell lines compared to controls over 96 h (Fig. 5B). The tumors with HOXB2 overexpressed grew significantly slower than the empty vector control JP1520 cell line (Fig. 5C and D), consistent with HOXB2 regulating growth specifically in the tumor microenvironment.

There were an increased percentage of cells in mitosis in the HOXB2 shRNA tumors and decreased mitosis in the HOXB2 ORF tumors compared to the empty vector controls (Fig. 6). Similar results were seen for the MTLn3-HOXB2 overexpressors. We saw no difference in apoptosis in the primary tumor as indicated by terminal deoxynucleotidyl transferase mediated-dUTP nick end labeling (TUNEL) staining in the tumor parenchyma (data not shown). We evaluated *in vitro* proliferation with 7-Aminoactinomycin D (7AAD) cell cycle analysis using MODFIT software (BrdU was also done, data not shown) and saw no significant difference compared to the parental MDA-MB 231 and SERPINE1-A control cell lines (Supplemental Fig. 2A and B). We saw no difference in *in vitro* survival with HOXB2 knockdown as indicated by annexin V staining (Supplemental Fig. 2C). We conclude that the increase in tumor growth with HOXB2 knockdown, and decreased growth with overexpression is attributable to changes in proliferation that are revealed in the tumor microenvironment.

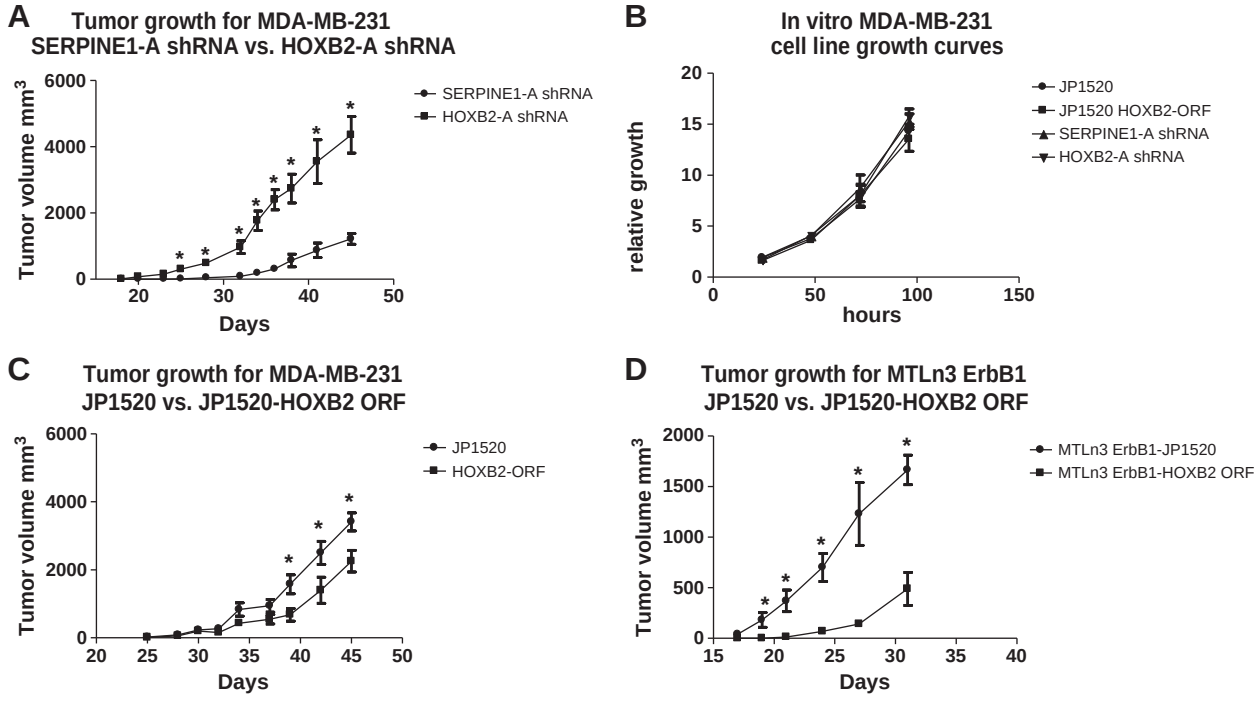

Fig. 5. HOXB2 negatively regulates tumor growth. (A) HOXB2-A shRNA cell line tumors grew faster than the control SERPINE1-A pGipz cell line. 1×10^6 cells were injected into the mammary fat pads of female SCID mice. Two separate injections of 5 and/or 4 mice were performed for each cell line. Tumors were measured and volumes calculated in mm^3 every 3 days for 45 days. Data represent the mean and SEM of 10 mice for the SERPINE1-A shRNA transductant line and 9 mice for the HOXB2-A shRNA transductant line. Stars represent $p \leq 0.05$ at the indicated time points. At 45 days, $p \leq 0.000181$. (B) HOXB2 has no effect on *in vitro* growth over 96 h. The HOXB2-ORF, JP1520 vector control, HOXB2-A shRNA, and SERPINE1-A cell lines were seeded in 6 well dishes at 50,000 cells per well and cells were counted in triplicate at 0 (first time point), 24, 48, 72, and 96 h from the first time point. Relative growth was calculated as a ratio of the average cell number at each time point to the initial average cell number at the first time point. *In vitro* growth assays were done in triplicate and repeated three times. Data are mean and SEM. There were no significant differences. (C) MDA-MB 231 HOXB2-ORF overexpression cell line tumors grew slower than the JP1520 vector control cell line. 1×10^6 cells were injected into the mammary fat pads of 10 female SCID mice, (two separate injections of 5 mice each, for each cell line). Tumors were measured and volumes calculated in mm^3 every 3 days for 45 days. Data represent the mean and SEM. Stars represent $p \leq 0.05$. At 45 days, $p \leq 0.00884$. (D) HOXB2 overexpression in MTLn3 rat adenocarcinoma cells decreased tumor growth. 5×10^5 cells were injected into the mammary fat pads of 5 female SCID mice for each cell line. Tumors were measured and volume was calculated over 30 days. Data shown are mean and SEM, stars represent p values $< .05$. At 31 days p value $= 0.000328049$.

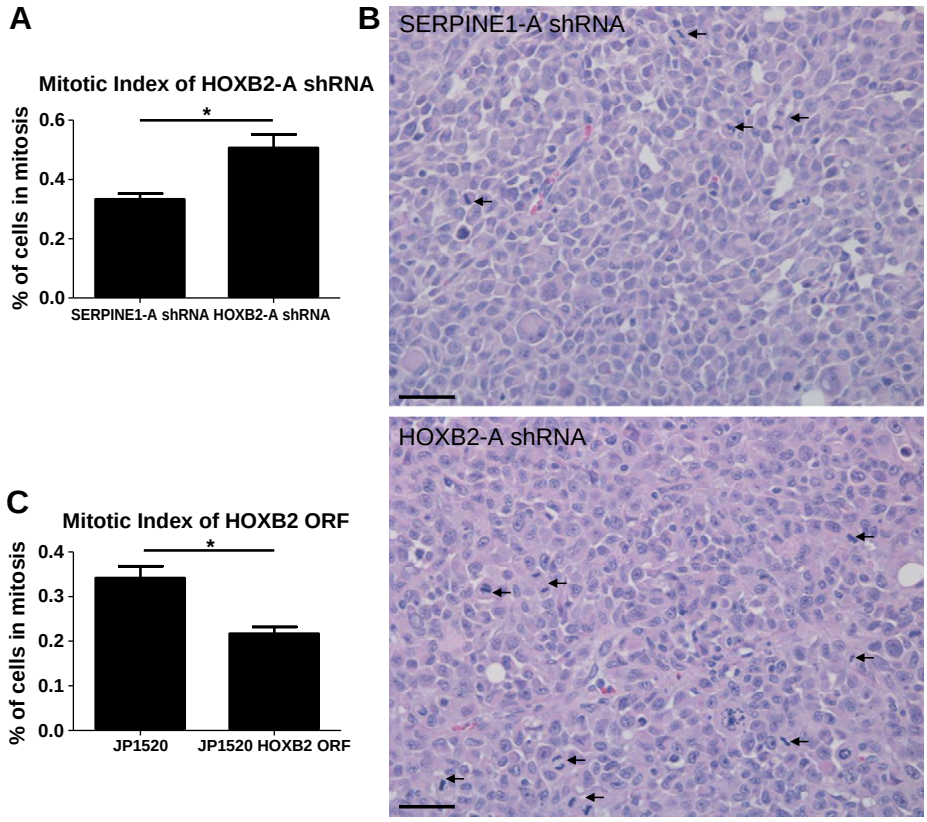

Fig. 6. HOXB2 affects the mitotic index of MDA-MB 231 tumors. Mitotic figures were counted in H&E tumor sections using a 40× objective in 10 random fields. N = 5 tumors for each cell line. For the shRNA lines: SERPINE1-A control vs. HOXB2-A p value = 0.015648318. For the overexpressor lines: JP1520 empty vector control vs. HOXB2 ORF p value = 0.00537099. Scale bar = 25 μm.

3. Discussion

In this study we performed an *in vivo* shRNA screen and were able to determine the changes in proportion of the knockdown cell lines after selection for *in vivo* tumor growth as well as seeding and growth in lung metastases after tail vein injection. The processes of tumor growth and metastasis are very sensitive to the *in vivo* architecture and microenvironment, making screens such as this important in elucidating the *in vivo* specific roles of the particular proteins being studied.

To correlate and validate the results of the *in vivo* screen we evaluated individual cell lines whose proportions changed in the pooled screen population. We prioritized genes for evaluation whose proportion change coincided with our hypothesized prediction based on its correlation with patient prognosis in breast cancer microarray studies. We were able to identify representatives of two categories of genes: genes which affect *in vivo* growth both in a mixture of cell lines and individually (HOXB2), and genes which differentially affect *in vivo* growth of tumor cells depending on whether the cells are in competition with other tumor cells (CYBA).

Knockdown of HOXB2 in two different breast cancer cell lines (MDA-MB-231 and T47D) resulted in increased primary tumor growth. Conversely, overexpression of the HOXB2 ORF in MDA-MB-231 and MTLn3-ErbB1 breast cancer lines reduced primary tumor growth. However, the effects on *in vitro* growth properties were not significantly different from control, indicating an *in vivo* specific effect that may be dependent on the tumor microenvironment. We did find a small but significant increase in invasiveness of cells suppressed in expression of HOXB2, and it is possible that the increased invasion may contribute to the increased *in vivo* growth rate. HOXB2 is part of the homeobox family of genes, which are important in normal vertebrate limb and organ development [13–16]. Overexpression of various homeobox genes have been correlated with lung, ovarian, cervical, and breast cancer progression [17–22]. However, HOX genes can also function in a tumor suppressor role in prostate and bladder cancer [23,24]. In breast cancer, the HOXA5 gene was shown to regulate p53 transcription, with its methylation/silencing resulting in down-regulation of p53 expression and subsequent p53 mediated malignant transformation [25]. The HOX genes function in a delicate balance, with either overexpression or downregulation causing transformation depending on the specific HOX gene and tissue specificity. Our results are particularly interesting in that they demonstrate an *in vivo* function for HOXB2 that was not detectable by *in vitro* assays.

Our results are at odds with previous HOXB2 studies in pancreatic, lung, and cervical cancer where overexpression was associated with malignancy [21,22,26]. However, breast cancer data in the Oncomine [27] and KMPlot [28] databases support our analysis. Overexpression of HOXB2 was correlated with a better prognostic outcome: Kaplan Meier plots from breast cancer patients indicate that overexpression of HOXB2 correlates with longer relapse free survival. HOXB2 expression was significantly increased ($p<.05$) in estrogen receptor positive tumors in 17 out of 21 microarray studies, and HOXB2 is more highly expressed in estrogen receptor positive cell lines compared to more aggressive, estrogen negative cell lines [29]. HOXB2 was significantly underexpressed in higher grade tumors: using Oncomine to perform a Grade Analysis for HOXB2 in breast cancer, HOXB2 expression was significantly lower ($p<.05$) in Grade 3 tumors in 7 out of the 14 microarray studies present ($p<.00001$[27]). Our observations that reducing HOXB2 expression increases mitosis figures and tumor growth *in vivo* are consistent with the observed effects on grade and outcome.

We identified a larger number of candidate genes in the *in vivo* tumor screen compared to the experimental lung metastasis screen. This may indicate the importance of paracrine interactions between cells in the tumor microenvironment, where cells interact closely in a mixed population, compared to tail vein injection where individual clones may seed in the lung and grow out in relative isolation. Paracrine signaling between cells could provide a selective pressure in the developing tumor, and an exciting outcome of this screen is the possibility of identifying genes needed for competition within the developing tumor cell population but which do not alter tumor growth in a clonal population. Previous studies have explored the evolving heterogeneity in the tumor microenvironment [30,31]. We have identified the CYBA gene as a gene that may provide a selective advantage in the heterogeneous, developing tumor microenvironment. Although the CYBA knockdown line on its own showed normal growth rates, when present in either the original pool or in varied mixtures (Supplemental Fig. 5), with the control line, its representation was significantly reduced. The concept of genes which are correlated with prognosis and alter the ability of a proportion of cells expressing this gene at a particular level to compete with other cells in the tumor microenvironment is novel and could be elaborated on using the methods we describe.

Our studies also indicate limitation of this approach given current technology. Many of the shRNA vectors did not provide efficient knockdown of our target genes, and it was often a challenge to find at least one knockdown above 50% to use in the screen. Another unexpected result was our finding that the shRNA advertised as being a non-targeting control (CT1) increased almost 10 fold after tumor growth in the screen, and this result was validated evaluating the individual cell line. This indicates that this non-targeting shRNA most likely had an off target effect, since other cell lines such as SERPINE1-A and TGBI-C grew similarly to the parental cell line and each other (Table 2). Thus further improvements in the selection of knockdown sequences and development of vectors for suppression would be valuable. In addition, although we noted that lines with reduced expression of potential positive effectors ID1, VCAM1, EREG, and IL13RA2 decreased in proportion during primary tumor growth, correlating with previous studies [32,33], we did not see a significant decrease in these lines or lines with reduced expression of EGFR or RHOC in the experimental lung metastasis screen. This is inconsistent with previous work showing VCAM1, IL13RA2, and ID1 were important for lung metastasis [11,32,33]. There are several possible explanations for this difference. These discrepancies may be due to: 1) lower knockdown efficiencies in some cases (ID-1 and EGFR), 2) differences in the MDA-MB-231 subline used, (clone 4173 in our study vs. the 4175 clone previously characterized), or 3) different methods used to measure metastasis (histology in our study vs. bioluminescence). While RHOC has been shown to be important for metastasis in breast cancer [34,35], it has not been previously characterized as necessary for MDA-MB-231 *in vivo* metastasis or specifically shown to affect the metastatic ability of the 4173 clone.

In summary, our studies demonstrate the value of using *in vivo* approaches to identify genes whose contributions to breast cancer malignancy may be difficult to identify *in vitro*. Our data indicate that the tumor microenvironment, as determined both by the different types of stromal cells present as well as the heterogeneity of the tumor cell population that evolves during tumor progression, plays a role in selecting for the expression of genes which are then correlated with patient outcome.

4. Materials and methods

4.1. Tissue culture

The parental MDA-MB-231 cells were derived from the pleural effusion of a breast cancer patient [36]. Clone 4173, kindly provided by Joan Massague, was identified as being highly metastatic, specifically to the lungs, after *in vivo* selection of parental MDA-MB-231 cells for lung metastasis [11]. All the studies with MDA-MB-231 cells described in this paper were performed with the 4173 clone. MDA-MB-231 cell lines were cultured in DMEM (Cellgro, Manassas, VA), 10% fetal bovine serum, FBS (S11550 Atlanta Biologicals, Lawrenceville, GA), and penicillin (100 units/ml)-streptomycin (0.1 mg/ml). MTLn3-ErbB1 rat adenocarcinoma cells expressing ErbB1 [12] were cultured in alpha MEM, 5% FBS. All cell lines were cultured at 37 °C and 5% CO_2. To generate the individual shRNA transductant cell lines, pGipz shRNA GFP lentiviral vectors (Supplemental Table 1, Open Biosystems, Huntsville, AL) were transfected into HEK 293T/17 cells (American Type Culture Collection) with packaging vectors TAT, REV, GAG/POL and VSV-G using Fugene 6 Transfection Reagent (11 815 091 001, Roche, Indianapolis, IN). Tumor cells were transduced with supernatants containing virus in the presence of polybrene (8 μg/ml) and placed under puromycin selection (1 μg/ml) for 2 weeks. The JP1520 empty control vector and HOXB2 cDNA retroviral vectors were obtained from the Dana-Farber/Harvard Cancer Center DNA Resource Core and were transfected into Phoenix cells (kindly provided by Dr. Gary P. Nolan) using Fugene 6. The supernatant was used to transduce tumor cells with polybrene (8 μg/ml) and selected for puromycin resistance as above. To make the pooled population the twenty five individual shRNA cell lines were counted and combined in equal proportions in groups of 5. The five groups were then combined into one large pool and grown to 80% confluence on 15 cm dishes for isolation of gDNA from the initial pool, *in vivo* injections, *in vitro* growth, and storage of stocks.

For *in vitro* growth, the initial pool was split 1:5, 3 times per week in the absence of puromycin. These cultures were placed under puromycin selection after 4 and 6 weeks of *in vitro* growth in parallel to the isolation and plating of *in vivo* samples in puromycin. gDNA was isolated at 4 weeks (corresponding to the times for experimental lung metastasis analyses using tail vein injection), and 6 weeks (corresponding to orthotopic primary tumor growth and spontaneous metastasis using mammary fat pad injection).

4.2. RNA extraction, PCR amplification, and real-time PCR to evaluate gene expression

To evaluate gene expression in the individual cell lines (Supplemental Table 1), RNA was isolated from ~70% confluent 10 cm dishes using the RNeasy mini kit, (74104, Qiagen, Valencia, CA). DNA was digested with RNase free DNase (79254, Qiagen, Valencia, CA). One microgram of total RNA was reverse transcribed into cDNA using the Superscript III first strand synthesis kit, (11752-050, Invitrogen, Carlsbad, CA). 100 ng of cDNA was evaluated with SABiosciences qRT-PCR Primer Assay sets for each gene (Supplemental Table 2). qRT-PCR was performed in triplicate using SYBR green master mix (PA-012, SAbiosciences, Frederick, MD) and a two-step cycling program (supplemental materials and methods), for the Applied Biosystems 7900HT. Results were evaluated with ABI Prism SDS 2.1 software, and the mean threshold cycle (C_T) values were used for analysis. To determine the expression levels of each gene the average C_T was compared to the GAPDH housekeeping gene (SAbiosciences, qRT-PCR Primer Assay PPH00150E).

4.3. Animal models

All procedures involving mice were conducted in accordance with the National Institutes of Health regulations concerning the use and care of experimental animals and were approved by the Albert Einstein College of Medicine animal use committee. The pool of shRNA transductants, or MDA-MB-231 individual shRNA cell lines (for growth evaluation) was grown to 80% confluence and detached with PBS containing 2 mM EDTA. One million cells in PBS, .7% Bovine Serum Albumin (w/v), BSA, and 20% (v/v) type I collagen (354249,

Becton Dickinson, Franklin Lakes, NJ), were injected into the right fourth mammary fat pad from the head of 5 to 7 week old female severe combined immunodeficient (SCID) mice (National Cancer Institute, Frederick, MD). MTLn3 ErbB1 JP1520 and MTLn3 ErbB1 HOXB2 ORF cell lines were detached in PBS, 2 mM EDTA and 1×10^6 cells resuspended in PBS, 0.35% BSA for injection into the mammary fat pads of 5 female SCID mice per line to evaluate growth. Injections of the pool were done at two separate times with 5 mice and then 4 mice to account for any injection differences. After six weeks of growth, when tumors reached 1.5 to 2 cm in diameter, they were removed for evaluation of transductant proportions in the screen.

For *in vivo* primary tumor growth analysis of individual cell lines, tumor growth rate was monitored at weekly intervals by measuring in two dimensions, and tumor volumes were calculated using the formula: length$\times$width^2/2. Tumors were measured every 3 days starting from day 18 post injection, for up to 58 days. After growth analysis tumors were fixed in 10% neutral formalin buffer, embedded in paraffin, sectioned at 5 μm and stained by H&E. Mitotic figures were counted in each field using a 20× objective in tumor sections taken from samples grown for 6 weeks. Mitotic figures were counted for 5 tumors per line in 10 random fields of healthy tumor parenchyma. Total numbers of cells were counted per field and the percentage of cells in mitosis was calculated as the number of cells in mitosis/the total number of cells$\times$100.

To evaluate growth and seeding in lung metastases, the pool of shRNA transductants was detached with PBS 2 mM EDTA and 1×10^6 cells in PBS (-Ca/-Mg) were injected into the lateral tail vein of female SCID mice. After 4 weeks the lungs were removed for evaluation of lung metastasis. The degree of lung metastasis was evaluated immediately after dissection using a fluorescence dissecting microscope to evaluate surface GFP fluorescent lung metastases. Lungs containing at least 1000 metastases were used for further analysis. For individual cell line evaluation of lung seeding and growth 2.5×10^5 cells were injected into the tail veins of SCID mice and after 3 weeks lungs were fixed in 10% neutral formalin buffer, embedded in paraffin, sectioned at 5 μm and stained by H&E. For each lung sample, metastases were counted using a 20× objective.

4.4. Genomic DNA isolation, and qRT-PCR analysis to evaluate pool proportions

Lungs and primary tumors were chopped into small pieces, washed in PBS, and dissociated in PBS with collagenase type IV (6 mg/ml, C5138, Sigma, St. Louis, MO), hyaluronidase (1 mg/ml, H3506 Sigma), and DNase I (0.25 mg/ml, D5025-15KU, Sigma) for 30 min with continuous agitation at 37 °C. Following digestion, samples were washed twice in sterile PBS. A minimum of at least 100,000 resistant cells grew out from the *in vivo* samples cultured under puromycin selection. gDNA was isolated from samples for subsequent analysis after no longer than one week in culture when 100 mm dishes were about 70% confluent (DNeasy kit 69504, Qiagen, Valencia, CA). The *in vitro* injected pool was cultured in parallel during the *in vivo* growth steps without puromycin selection and then was also grown under puromycin selection in parallel with the cells isolated from the *in vivo* samples.

Unique barcode sequences for each of the pGipz shRNA vectors were sequenced using the sequencing primer GCATTAAAGCAGCGTATC. To analyze changes in the proportions of individual transductants after growth *in vivo*, qRT-PCR barcode reverse primers were designed with Primer 3 software, specific to each individual barcode (Supplemental Table 3) [8]. A common forward primer was used (Supplemental Table 3). Primers were designed based on qRT-PCR primer parameters and tested with qRT-PCR of the individual cell line's gDNA, prior to their use in the screen. Specific barcode primers were aligned using the EMBOSS Pairwise Alignment Algorithm [37], with other cell line barcodes and sequences. Primers with alignment scores above 60% similarity to other barcodes were evaluated for mispriming to test the specificity of each of the primer sets. 100 ng of total gDNA and 500 nM of primers (common forward and specific barcode reverse primer), were used for each triplicate reaction. For each gDNA sample, the level of the endogenous beta actin gene was used to normalize to total genomic DNA (Suppl. Table 3), by subtracting the beta actin C_T from the barcode C_T, producing a ΔC_T using the average C_T of the triplicate reactions. The change in representation of each barcode between two samples was calculated as a $\Delta\Delta C_T$: the difference between the ΔC_T's for that barcode of the two populations being compared. The C_T values for all transductants in the *in vivo* and *in vitro* samples were measured at least twice on different days done in triplicate for each qRT-PCR reaction.

4.5. Selection of genes for screening

To evaluate which genes to use in the screen, three microarray studies, correlating gene expression with patient survival, were used for analysis [2,4,5]. p Values were generated in a *t*-test comparing the median difference in expression of a particular gene between patients surviving >5 years vs. <5 years in each study. The median of the p values for a particular gene across all three microarray studies was used to generate a list of genes whose expression is correlated positively (potential tumor growth or metastasis suppressor), or negatively (potential tumor growth or metastasis enhancer) with survival. The top twenty five genes (with the lowest median p value) were selected for development of an *in vivo* metastasis screen, (Supplemental Table 1). Their correlation with survival was also confirmed in the Oncomine microarray database. Utilizing the data in [29], the average level of expression of the selected genes in MDA-MB-231 cells is similar to the other breast cancer cell lines (mean and SEM of the ratio 1.02 +/− .03). Potential positive controls in the screen were genes (ID1, IL13RA2, and VCAM1, EREG, EGFR) shown previously to be mediators of growth or metastasis and correlated with poor prognosis [11,12,33]. A non-targeting shRNA from Openbiosystems, CT-1, was used as a negative control.

Supplementary materials related to this article can be found online at doi:10.1016/j.ygeno.2011.05.011.

Acknowledgments

We thank Dr. Joan Massague for providing MDA-MB-231 clone 4173, and the Cox, Condeelis, Hodgson and Segall labs for comments and suggestions. This work was supported by a Breast Cancer Alliance Exceptional Project Award, CA125288, and CA077522 to J.E.S. J.E.S. is the Betty and Sheldon Feinberg Senior Faculty Scholar in Cancer Research.

References

[1] G.P. Gupta, J. Massague, Cancer metastasis: building a framework, Cell 127 (2006) 679–695.
[2] M.J. van de Vijver, Y.D. He, L.J. van't Veer, H. Dai, A.A. Hart, D.W. Voskuil, G.J. Schreiber, J.L. Peterse, C. Roberts, M.J. Marton, M. Parrish, D. Atsma, A. Witteveen, A. Glas, L. Delahaye, T. van der Velde, H. Bartelink, S. Rodenhuis, E.T. Rutgers, S.H. Friend, R. Bernards, A gene-expression signature as a predictor of survival in breast cancer, N. Engl. J. Med. 347 (2002) 1999–2009.
[3] L.J. van't Veer, H. Dai, M.J. van de Vijver, Y.D. He, A.A. Hart, M. Mao, H.L. Peterse, K. van der Kooy, M.J. Marton, A.T. Witteveen, G.J. Schreiber, R.M. Kerkhoven, C. Roberts, P.S. Linsley, R. Bernards, S.H. Friend, Gene expression profiling predicts clinical outcome of breast cancer, Nature 415 (2002) 530–536.
[4] A.H. Bild, G. Yao, J.T. Chang, Q. Wang, A. Potti, D. Chasse, M.B. Joshi, D. Harpole, J.M. Lancaster, A. Berchuck, J.A. Olson Jr., J.R. Marks, H.K. Dressman, M. West, J.R. Nevins, Oncogenic pathway signatures in human cancers as a guide to targeted therapies, Nature 439 (2006) 353–357.
[5] K. Chin, S. DeVries, J. Fridlyand, P.T. Spellman, R. Roydasgupta, W.L. Kuo, A. Lapuk, R.M. Neve, Z. Qian, T. Ryder, F. Chen, H. Feiler, T. Tokuyasu, C. Kingsley, S. Dairkee, Z. Meng, K. Chew, D. Pinkel, A. Jain, B.M. Ljung, L. Esserman, D.G. Albertson, F.M. Waldman, J.W. Gray, Genomic and transcriptional aberrations linked to breast cancer pathophysiologies, Cancer Cell 10 (2006) 529–541.

[6] A.M. Glas, A. Floore, L.J. Delahaye, A.T. Witteveen, R.C. Pover, N. Bakx, J.S. Lahti-Domenici, T.J. Bruinsma, M.O. Warmoes, R. Bernards, L.F. Wessels, L.J. Van't Veer, Converting a breast cancer microarray signature into a high-throughput diagnostic test, BMC Genomics 7 (2006) 278.
[7] F. Cardoso, L. Van't Veer, E. Rutgers, S. Loi, S. Mook, M.J. Piccart-Gebhart, Clinical application of the 70-gene profile: the MINDACT trial, J. Clin. Oncol. 26 (2008) 729–735.
[8] J.M. Silva, K. Marran, J.S. Parker, J. Silva, M. Golding, M.R. Schlabach, S.J. Elledge, G.J. Hannon, K. Chang, Profiling essential genes in human mammary cells by multiplex RNAi screening, Science 319 (2008) 617–620.
[9] M.R. Schlabach, J. Luo, N.L. Solimini, G. Hu, Q. Xu, M.Z. Li, Z. Zhao, A. Smogorzewska, M.E. Sowa, X.L. Ang, T.F. Westbrook, A.C. Liang, K. Chang, J.A. Hackett, J.W. Harper, G.J. Hannon, S.J. Elledge, Cancer proliferation gene discovery through functional genomics, Science 319 (2008) 620–624.
[10] L. Zender, W. Xue, J. Zuber, C.P. Semighini, A. Krasnitz, B. Ma, P. Zender, S. Kubicka, J.M. Luk, P. Schirmacher, W.R. McCombie, M. Wigler, J. Hicks, G.J. Hannon, S. Powers, S.W. Lowe, An oncogenomics-based in vivo RNAi screen identifies tumor suppressors in liver cancer, Cell 135 (2008) 852–864.
[11] A.J. Minn, G.P. Gupta, P.M. Siegel, P.D. Bos, W. Shu, D.D. Giri, A. Viale, A.B. Olshen, W.L. Gerald, J. Massague, Genes that mediate breast cancer metastasis to lung, Nature 436 (2005) 518–524.
[12] C. Xue, J. Wyckoff, F. Liang, M. Sidani, S. Violini, K.L. Tsai, Z.Y. Zhang, E. Sahai, J. Condeelis, J.E. Segall, Epidermal growth factor receptor overexpression results in increased tumor cell motility in vivo coordinately with enhanced intravasation and metastasis, Cancer Res. 66 (2006) 192–197.
[13] P. Dolle, J.C. Izpisua-Belmonte, J. Brown, C. Tickle, D. Duboule, Hox genes and the morphogenesis of the vertebrate limb, Prog. Clin. Biol. Res. 383A (1993) 11–20.
[14] G. Zacchetti, D. Duboule, J. Zakany, Hox gene function in vertebrate gut morphogenesis: the case of the caecum, Development 134 (2007) 3967–3973.
[15] W.V. Cardoso, Transcription factors and pattern formation in the developing lung, Am. J. Physiol. 269 (1995) L429–L442.
[16] N. Shah, S. Sukumar, The Hox genes and their roles in oncogenesis, Nat. Rev. Cancer 10 (2010) 361–371.
[17] M. Abe, J. Hamada, O. Takahashi, Y. Takahashi, M. Tada, M. Miyamoto, T. Morikawa, S. Kondo, T. Moriuchi, Disordered expression of HOX genes in human non-small cell lung cancer, Oncol. Rep. 15 (2006) 797–802.
[18] J. Miao, Z. Wang, H. Provencher, B. Muir, S. Dahiya, E. Carney, C.O. Leong, D.C. Sgroi, S. Orsulic, HOXB13 promotes ovarian cancer progression, Proc. Natl. Acad. Sci. U.S.A. 104 (2007) 17093–17098.
[19] Y. Zhai, R. Kuick, B. Nan, I. Ota, S.J. Weiss, C.L. Trimble, E.R. Fearon, K.R. Cho, Gene expression analysis of preinvasive and invasive cervical squamous cell carcinomas identifies HOXC10 as a key mediator of invasion, Cancer Res. 67 (2007) 10163–10172.
[20] X. Wu, H. Chen, B. Parker, E. Rubin, T. Zhu, J.S. Lee, P. Argani, S. Sukumar, HOXB7, a homeodomain protein, is overexpressed in breast cancer and confers epithelial–mesenchymal transition, Cancer Res. 66 (2006) 9527–9534.
[21] K. Inamura, Y. Togashi, M. Okui, H. Ninomiya, M. Hiramatsu, Y. Satoh, S. Okumura, K. Nakagawa, T. Shimoji, T. Noda, Y. Ishikawa, HOXB2 as a novel prognostic indicator for stage I lung adenocarcinomas, J. Thorac. Oncol. 2 (2007) 802–807.
[22] R. Lopez, E. Garrido, P. Pina, A. Hidalgo, M. Lazos, R. Ochoa, M. Salcedo, HOXB homeobox gene expression in cervical carcinoma, Int. J. Gynecol. Cancer 16 (2006) 329–335.
[23] C. Jung, R.S. Kim, H.J. Zhang, S.J. Lee, M.H. Jeng, HOXB13 induces growth suppression of prostate cancer cells as a repressor of hormone-activated androgen receptor signaling, Cancer Res. 64 (2004) 9185–9192.
[24] C.J. Marsit, E.A. Houseman, B.C. Christensen, L. Gagne, M.R. Wrensch, H.H. Nelson, J. Wiemels, S. Zheng, J.K. Wiencke, A.S. Andrew, A.R. Schned, M.R. Karagas, K.T. Kelsey, Identification of methylated genes associated with aggressive bladder cancer, PLoS One 5 (2010).
[25] V. Raman, S.A. Martensen, D. Reisman, E. Evron, W.F. Odenwald, E. Jaffee, J. Marks, S. Sukumar, Compromised HOXA5 function can limit p53 expression in human breast tumours, Nature 405 (2000) 974–978.
[26] D. Segara, A.V. Biankin, J.G. Kench, C.C. Langusch, A.C. Dawson, D.A. Skalicky, D.C. Gotley, M.J. Coleman, R.L. Sutherland, S.M. Henshall, Expression of HOXB2, a retinoic acid signaling target in pancreatic cancer and pancreatic intraepithelial neoplasia, Clin. Cancer Res. 11 (2005) 3587–3596.
[27] Oncomine™ (Compendia Bioscience), https://www.oncomine.org, January 2010, in, Ann Arbor, MI.
[28] B. Gyorffy, A. Lanczky, A.C. Eklund, C. Denkert, J. Budczies, Q. Li, Z. Szallasi, An online survival analysis tool to rapidly assess the effect of 22,277 genes on breast cancer prognosis using microarray data of 1,809 patients, Breast Cancer Res. Treat. 123 (2010) 725–731.
[29] R.M. Neve, K. Chin, J. Fridlyand, J. Yeh, F.L. Baehner, T. Fevr, L. Clark, N. Bayani, J.P. Coppe, F. Tong, T. Speed, P.T. Spellman, S. DeVries, A. Lapuk, N.J. Wang, W.L. Kuo, J.L. Stilwell, D. Pinkel, D.G. Albertson, F.M. Waldman, F. McCormick, R.B. Dickson, M.D. Johnson, M. Lippman, S. Ethier, A. Gazdar, J.W. Gray, A collection of breast cancer cell lines for the study of functionally distinct cancer subtypes, Cancer Cell 10 (2006) 515–527.
[30] S.Y. Park, M. Gonen, H.J. Kim, F. Michor, K. Polyak, Cellular and genetic diversity in the progression of in situ human breast carcinomas to an invasive phenotype, J. Clin. Invest. 120 (2010) 636–644.
[31] S.Y. Park, H.E. Lee, H. Li, M. Shipitsin, R. Gelman, K. Polyak, Heterogeneity for stem cell-related markers according to tumor subtype and histologic stage in breast cancer, Clin. Cancer Res. Official J. Am. Assoc. Cancer Res. 16 (2010) 876–887.
[32] C.Q. Lin, J. Singh, K. Murata, Y. Itahana, S. Parrinello, S.H. Liang, C.E. Gillett, J. Campisi, P.Y. Desprez, A role for Id-1 in the aggressive phenotype and steroid hormone response of human breast cancer cells, Cancer Res. 60 (2000) 1332–1340.
[33] P.Y. Desprez, C.Q. Lin, N. Thomasset, C.J. Sympson, M.J. Bissell, J. Campisi, A novel pathway for mammary epithelial cell invasion induced by the helix–loop–helix protein Id-1, Mol. Cell. Biol. 18 (1998) 4577–4588.
[34] A. Hakem, O. Sanchez-Sweatman, A. You-Ten, G. Duncan, A. Wakeham, R. Khokha, T.W. Mak, RhoC is dispensable for embryogenesis and tumor initiation but essential for metastasis, Genes Dev. 19 (2005) 1974–1979.
[35] T. Kusama, M. Mukai, M. Tatsuta, H. Nakamura, M. Inoue, Inhibition of transendothelial migration and invasion of human breast cancer cells by preventing geranylgeranylation of Rho, Int. J. Oncol. 29 (2006) 217–223.
[36] R. Cailleau, M. Olive, Q.V. Cruciger, Long-term human breast carcinoma cell lines of metastatic origin: preliminary characterization, In Vitro 14 (1978) 911–915.
[37] European Bioinformatics Institute, http://www.ebi.ac.uk/Tools/emboss/align/, January 2010, in.